ELSEVIER

Physica C 274 (1997) 295–303

PHYSICA C

Improved critical current density and irreversibility line in HIP'ed Chevrel phase superconductor $PbMo_6S_8$

H.D. Ramsbottom, D.P. Hampshire *

Department of Physics, University of Durham, Durham, UK

Received 29 July 1996; revised manuscript received 25 November 1996

Abstract

Flux penetration measurements have been made from 4.2 K up to T_c in DC magnetic fields up to 10 T on Hot Isostatically Pressed (HIP'ed) and unHIP'ed samples of $PbMo_6S_8$ (PMS). Fabricating at 2×10^8 $N m^{-2}$ increases the critical current density (J_c) by a factor of typically 20 to greater than 4×10^8 $A m^{-2}$ at 5 T and 6 K and the irreversibility line by a factor of almost 2, so that for HIP'ed PMS the irreversibility line lies very close to $\mu_0 H_{C2}(T)$ values determined from reversible DC magnetisation measurements. An analysis of the J_c data using Kramer's universal scaling law gives a calculated value of J_c at 10 T and 4.2 K of 4×10^8 $A m^{-2}$ and a value for the irreversibility field of 39 T at 4.2 K. It is suggested that the increase in J_c produced by the HIP process, is due to increasing the contact area between the grains by increasing the density, and improving the superconducting properties at the grain boundaries.

Keywords: Chevrel superconductors; Critical current; Hot isostatic press

1. Introduction

Since they were discovered over 20 years ago [1], Chevrel phase superconductors have been of great interest both as a potential material for new technological applications and for fundamental studies of superconductivity. With a T_c of 15 K [2] and an extremely high upper critical field, greater than 54 T [3–7], $PbMo_6S_8$ (PMS) is a candidate for high field applications [8,9]. If the critical current density (J_c) of PMS can be increased above the present state-of-the-art values in wires by a factor of four, PMS may be an essential component in the next generation of high field magnets operating above 20 T.

PMS has a coherence length of 2 nm [10,11], between that of the commercially important low temperature superconductors (5 nm) and that found in the *c*-direction of the high temperature superconductors (0.5 nm). It can provide a model system to develop an understanding of superconductors with short coherence length [12]. Improvements in the critical properties of PMS by advanced or novel materials processing techniques may lead to improvements in high temperature superconductors (HTS), where processing is considerably more complex.

This paper presents detailed variable temperature flux penetration measurements on PMS in high magnetic fields, following experimental procedures first developed by Campbell [13]. Using a purpose-built probe [14], results were obtained from 4.2 K up to T_c in magnetic fields up to 10 T. The results are used to

* Corresponding author. Fax: +44 191 374 3749.

PII S0921-4534(96)00684-3

measure the improvement in J_c and the irreversibility line achieved by fabricating PMS using a hot isostatic press (HIP). Hot isostatic pressing involves the simultaneous application of high pressure and high temperature to obtain a dramatic increase in density and improves other metallurgical properties such as fracture toughness, phase purity and grain boundary composition [15–19].

Section 2 describes the fabrication of the samples and preliminary characterisation using AC susceptibility and X-ray diffraction. Flux penetration measurements on the HIP'ed PMS sample and the sample produced at ambient pressure are presented in Section 3. Section 4 includes the central results of this work. The flux penetration data are analysed to find the magnetic field profiles, critical current densities, scaling relations and irreversibility lines. The paper ends with a discussion and summary of the improvements in the properties of the HIP'ed PMS sample.

2. Fabrication / preliminary characterisation

The detailed fabrication of the HIP'ed and unHIP'ed PMS samples has been described elsewhere [20]. Elemental powders were mixed in the stoichiometric ratio Pb:Mo:S 1:6:8 and reacted in a two step procedure. The powders were pressed into pellets, sealed under vacuum in a silica tube, then reacted in a tube furnace in flowing high purity argon at 450°C for 4 hours and then at 650°C for 8

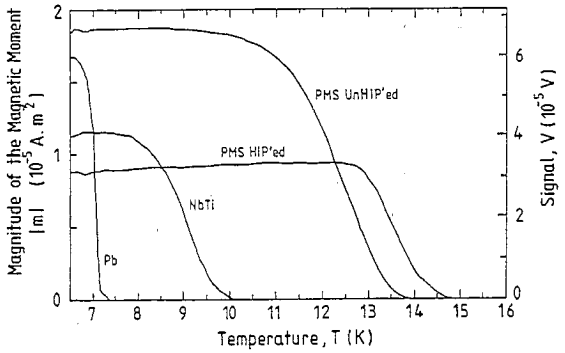

Fig. 1. The AC susceptibility of both unHIP'ed and HIP'ed $PbMo_6S_8$. For comparison data on a Pb and a NbTi sample are also shown.

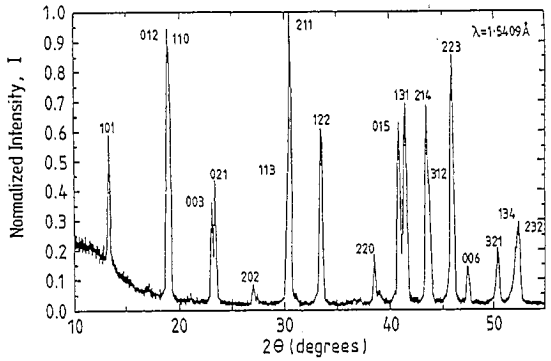

Fig. 2. The X-ray diffraction pattern for unHIP'ed $PbMo_6S_8$.

hours. They were then ground with a mortar and pestle in a glove box (< 10 ppm oxygen and water), pressed into pellets again and resealed under vacuum in silica. The pellets were then sintered for 44 hours at 1000°C. A (unHIP'ed) sample was cut from one of the sintered pellets with dimensions 2 mm × 2 mm × 6 mm. The remaining material was then wrapped in molybdenum foil, sealed under vacuum in a stainless steel envelope and placed in the HIP. The HIP cycle consisted of increasing the temperature to 800°C and the pressure to 2×10^8 Nm^{-2} (2000 bar). The temperature was maintained for 8 hours during which time the pressure reduced to 1.3×10^8 Nm^{-2}. A HIP'ed sample was then cut with dimensions 5 mm × 2.8 mm × 0.8 mm. Both the HIP'ed and unHIP'ed samples were characterised using AC susceptibility, X-ray diffraction (XRD) and scanning electron microscopy (SEM). Susceptibility measurements, shown in Fig. 1, were made using an AC field of 2 mT at a frequency of 19.7 Hz. The T_c of the HIP'ed sample is 13.5 K ($\Delta T_c \approx 1$ K), approximately 1 K higher and sharper than that of the unHIP'ed sample, with a T_c of 12.5 K ($\Delta T_c \approx 2$ K). The increase in T_c and reduction in the transition width has also been observed by Seeber [21]. Fig. 2 shows the XRD trace for the unHIP'ed sample. Similar results were found for the HIP'ed sample. All the major peaks can be attributed to PMS [22], which suggests that the samples are predominantly single phase. SEM observations show that the grain size is approximately 0.5–4 μm and demonstrates the marked increase in density, from less than 70% dense (unHIP'ed) to greater than 90% dense (HIP'ed). These results are typical of high quality PMS samples.

3. Experimental results

A purpose built probe has been designed for making variable temperature flux penetration measurements in high DC magnetic fields on bulk, high J_c materials. In principle, the apparatus is similar to that used in AC susceptibility measurements. However, the primary coil of the apparatus can produce large AC fields of up to 100 mT in large DC fields up to 17 T. The sample is situated in a secondary pick-up coil which incorporates a variable temperature enclosure and is centrally located in the primary coil. Detailed design features and preliminary raw data on these materials have been presented elsewhere [14,20]. In such measurements, at a particular DC field and temperature, the sample is exposed to an increasing AC magnetic field. At low AC fields, currents flow at the surface to oppose the magnetic field penetrating the sample, in agreement with Lenz's law. At intermediate AC fields, the sample is fully penetrated and currents flow throughout the entire sample, this produces a minimum in the magnetic moment m_{rms}(min). At very high AC fields, above those necessary to fully penetrate the sample, during most of the cycle the critical current density (J_c) flows throughout the entire sample and the magnetic moment remains constant. The magnetic moment only changes during those parts of the cycle when the AC field is at its maximum and minimum values when the current flow in the sample is reversed. The response of the sample is monitored at the frequency of the AC field using a Lock-In-

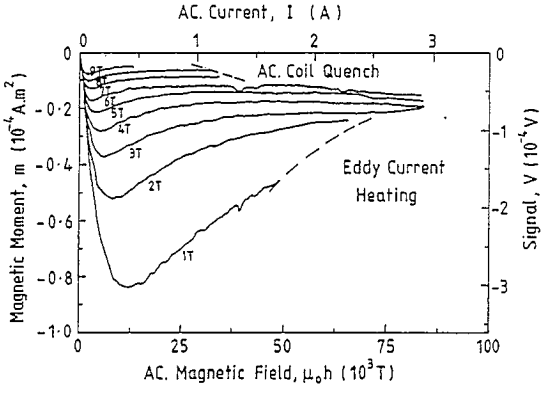

Fig. 3. Magnetic moment versus AC field for unHIP'ed $PbMo_6S_8$ as a function of DC field at 6 K.

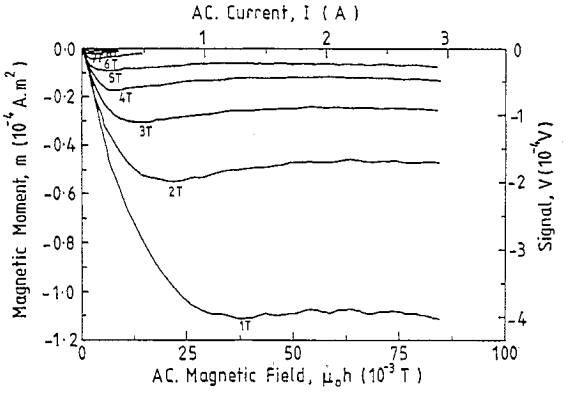

Fig. 4. Magnetic moment versus AC field for HIP'ed $PbMo_6S_8$ as a function of DC field at 11.7 K.

Amplifier (LIA). The rms voltage induced in the pick-up coil decreases to a minimum as the AC field fully penetrates the entire sample. As the AC field increases to very high values, since a voltage is only induced during part of the cycle, the rms voltage found by the LIA at the (fundamental) frequency of the AC field rises back to zero [23].

Figs. 3 and 4 show the magnetic moment versus AC field for both the unHIP'ed and HIP'ed samples of PMS as a function of DC field at 6 K and 11.7 K respectively. At low DC fields the maximum AC field is limited by requiring good temperature stability in the presence of Eddy current heating of the copper components of the probe. The maximum AC field which can be obtained at high DC fields is determined by quenching in the superconducting primary coil.

4. Analysis of results

4.1. Magnetic field profiles

Magnetic field profiles are calculated using the raw data in Figs. 3 and 4. The response of the sample is described using the formulism derived for a cylinder parallel to the DC and AC magnetic fields [23]. The depth the field penetrates into the sample (δ) can be approximated by,

$$\delta = r_m\left(1 - \frac{|dV_{rms}/dI_{rms}|}{|dV_{rms}/dI_{rms}|_{max}}\right), \qquad (1)$$

where V_{rms} is the rms voltage induced in the secondary pick-up coil by the sample, I_{rms} is the rms current in the primary coil, $|dV_{rms}/dI_{rms}|_{max}$ is the maximum value of $|dV_{rms}/dI_{rms}|$ found at low AC fields, and r_m is the radius of the cylinder, given by,

$$r_m = \left(\frac{\mu_0}{\pi} \frac{P}{LC} \left| \left(\frac{dV_{rms}}{dI_{rms}} \right) \right|_{max} \right)^{1/2}, \quad (2)$$

where L is the length of the sample, P is the probe constant (0.277 $A m^2 V^{-1}$ at 19.7 Hz) and C is the coil constant for the primary superconducting coil (28.7 $mT A^{-1}$). The probe constant (P) was determined by measuring a Pb sample of known geometry in the Meissner state. A Pb sample producing a rms magnetic moment of 1.66×10^{-5} $A m^2$ gave a rms voltage output at 19.7 Hz of 6.00×10^{-5} V. The coil constant (C) for the primary coil was measured using a calibrated Hall probe. A rigorous derivation of the penetration depth shows that Eq. (1) is correct to within a factor of 2 throughout the range $0 < \delta < r_m$ [23]. Equally the field inside the sample ($\mu_0 M$), can be determined from the magnetic field produced by the AC coil:

$$\mu_0 M = \sqrt{2}\, I_{rms} C. \quad (3)$$

Figs. 5 and 6 show the magnetic field profiles for both the unHIP'ed and HIP'ed sample of PMS as a function of DC field at 6 and 11.7 K. Eq. (2) gives $r_m \approx 1.2$ mm for the unHIP'ed sample which has dimensions orthogonal to the field of 2 mm × 2 mm.

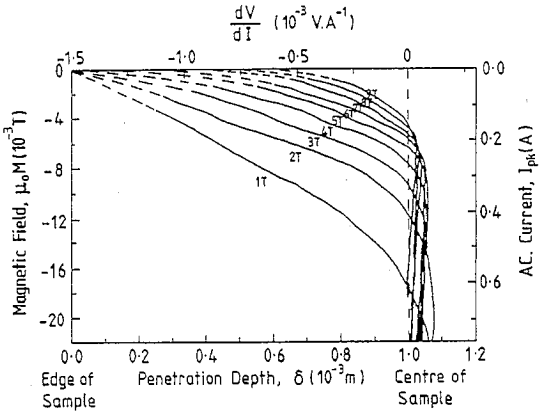

Fig. 5. The magnetic field profile inside unHIP'ed $PbMo_6S_8$ as a function of DC field at 6 K.

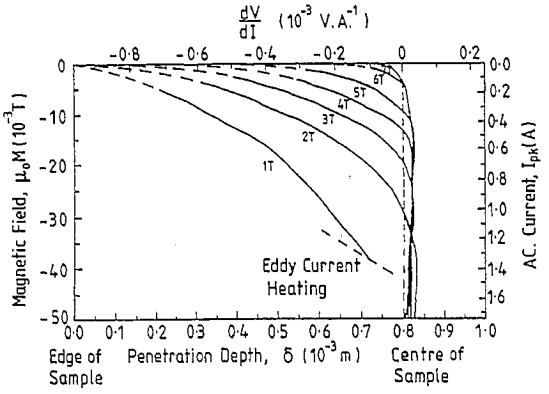

Fig. 6. The magnetic field profile inside HIP'ed $PbMo_6S_8$ as a function of DC field at 11.7 K.

For the HIP'ed sample, with equivalent dimensions 2.8 mm × 0.8 mm, Eq. (2) gives $r_m \approx 1$ mm. These values of r_m derived from magnetic measurements are consistent with geometrical dimensions measured with a micrometer, since Eqs. (1) and (2) are derived assuming a cylindrical geometry, where the value of the radius r_m effectively characterises the cross-sectional area of the sample (πr_m^2).

4.2. Critical current density

Bean's critical state model [24] can be extended to AC fields. At each field and temperature, the minimum value of the rms AC magnetic moment, $m_{rms}(\min)$, can be used to calculate an equivalent critical current density. In the standard expression relating the current density to the magnetic moment of a slab [25], the term for the magnetic moment is replaced by $\sqrt{2}\, m_{rms}(\min)$ to give [23],

$$J_c = \frac{2\sqrt{2}\, m_{rms}(\min)}{V^* a_2 (1 - a_2/(3a_1))}, \quad (4)$$

where V^* is the volume of the sample, and $2a_1$ and $2a_2$ ($a_1 > a_2$) are the width and thickness of the samples [23].

Figs. 7 and 8 show J_c values for the HIP'ed and unHIP'ed samples of PMS, calculated using Eq. (4). The values of J_c are accurate to within 20%, primarily due to the uncertainty in the dimensions of the samples. Alternatively, J_c can be calculated from the gradient of the magnetic field profiles using

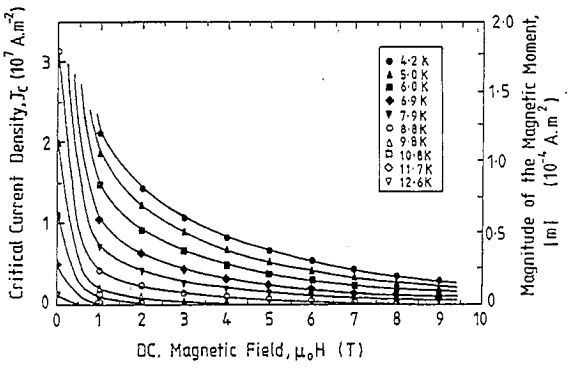

Fig. 7. The critical current density of unHIP'ed $PbMo_6S_8$ as a function of field and temperature.

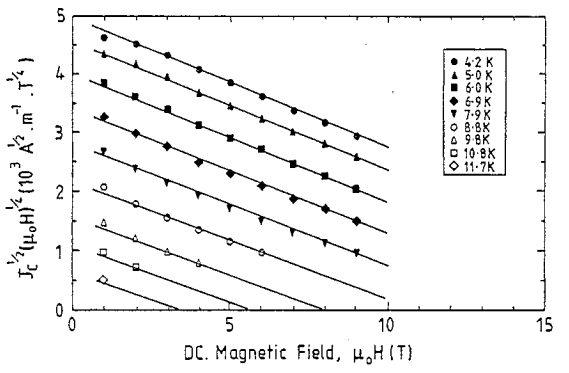

Fig. 9. A Kramer plot for unHIP'ed $PbMo_6S_8$.

Maxwell's equations (Figs. 5 and 6). However the non-cylindrical geometry and the approximations used to derive Eqs. (1) and (2) would lead to J_c values, uncertain to a factor of two or three. For the unHIP'ed sample, measurements were made at temperatures from 4.2 K and above. For the HIP'ed sample, measurements were made at temperatures of 6 K and above. Below 6 K, the AC field required to fully penetrate the HIP'ed sample is so large, that heating in the copper components of the probe prevent accurate temperature control. It can be seen from Figs. 7 and 8, that HIP'ing the PMS, has increased J_c typically by a factor of 20, giving a value of greater than 4×10^8 A m^{-2} at 5 T and 6 K.

4.3. Scaling relations and flux pinning

In Figs. 9 and 10, the data from Figs. 7 and 8 have been replotted using a Kramer plot [26]. A linear extrapolation of the data to $J_c^{1/2}(\mu_0 H)^{1/4} = 0$ gives the irreversibility field ($\mu_0 H_{irr}$) for each temperature. The volume pinning force is calculated using the equation $F_P = \mu_0(J_c \times H)$. For both samples the data can be described by a Kramer dependence of the form,

$$F_P = \alpha(\mu_0 H_{irr})^n h^{1/2}(1-h)^2, \qquad (5)$$

where h is the reduced magnetic field ($h = H/H_{irr}$) and α and n are constants.

From the data at high temperatures, the free parameters α and n have been calculated. The index $n = 2.36 \pm 0.11$ and 2.52 ± 0.11 and the constant $\alpha = 8.3 \times 10^4 T^{-1.36}$ A m^{-2} and $1.42 \times 10^6 T^{-1.52}$ A m^{-2}, for the unHIP'ed and HIP'ed samples of PMS respectively. These values of α and n have been used to calculate the irreversibility fields at those temperatures where few data are available, i.e. 10.8 and 11.7 K for the unHIP'ed sample and 6.0, 6.9 and 7.9 K for the HIP'ed sample.

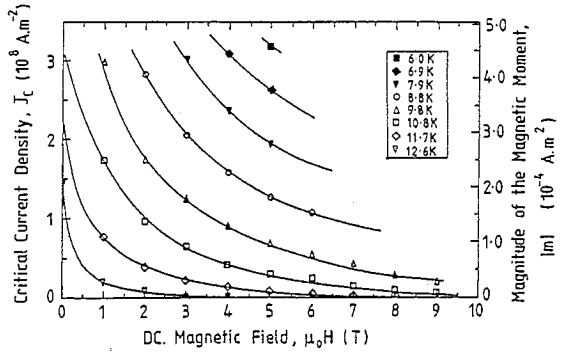

Fig. 8. The critical current density of HIP'ed $PbMo_6S_8$ as a function of field and temperature.

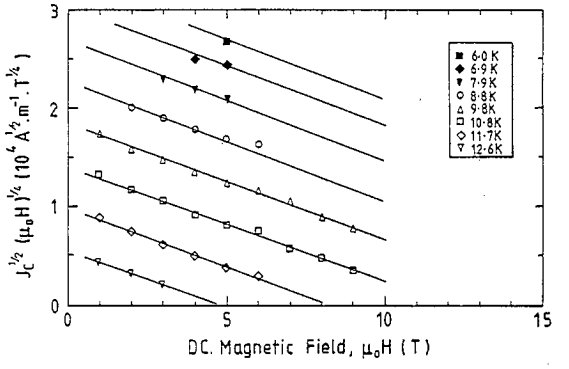

Fig. 10. A Kramer plot for HIP'ed $PbMo_6S_8$.

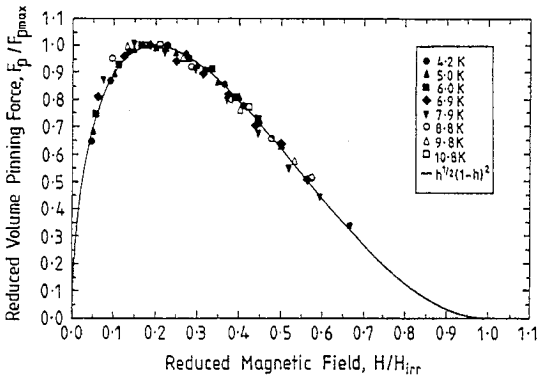

Fig. 11. The reduced volume pinning force versus the reduced magnetic field as a function of temperature for unHIP'ed $PbMo_6S_8$.

Figs. 11 and 12 show the data replotted as the reduced volume pinning force (F_P/F_{Pmax}) versus the reduced magnetic field ($h = H/H_{irr}$) as a function of temperature, where H_{irr} is taken from the Kramer plot. With the appropriate values of α and n, Eq. (5) has been used to calculate the solid lines in Figs. 11 and 12. To facilitate comparison with values in the literature, J_c is calculated to be (using the universal scaling law), 4×10^8 A m^{-2} at 4.2 K and 10 T.

Fig. 13 shows the irreversibility field plotted as a function of temperature for both unHIP'ed and HIP'ed PMS, consistent with the universal scaling law. The solid squares show values of $\mu_0 H_{C2}$ for HIP'ed PMS obtained from reversible DC magnetisation measurements. It can be seen that by HIP'ing

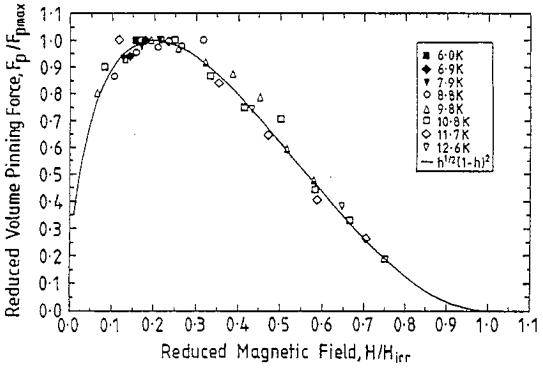

Fig. 12. The reduced volume pinning force versus the reduced magnetic field as a function of temperature for HIP'ed $PbMo_6S_8$.

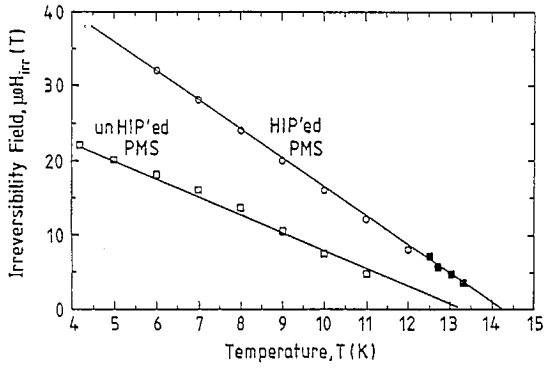

Fig. 13. The irreversibility field of $PbMo_6S_8$ as a function of temperature. (■) Values of the upper critical field obtained from reversible DC magnetisation measurements.

the sample, the irreversibility field at 4.2 K has increased by more than 15 T.

5. Discussion

The magnetic field profiles in Figs. 4 and 5 are consistent with a homogeneous superconductor with uniform pinning. At low penetration depths, the slope of the profiles is approximately proportional to J_c. The apparent penetration of the magnetic field to a distance greater than the sample radius has been shown to be an artifact of the harmonic analysis [23]. Rossel et al. [27] and Karasik et al. [28] have also made flux penetration measurements on PMS which indicate that the spatial variation of J_c is small. Cattani et al. [29,30] also found that the magnetic field profiles in their PMS samples never showed the two gradients characteristic of a granular sample, i.e. a sample with both an inter and intragranular J_c. However when PMS is encased with a barrier such as Mo to form a wire, a steep gradient is seen in the magnetic field profile at low δ [31]. This is attributed to surface pinning at the superconducting–normal interface. Le Lay et al. concluded that despite the short coherence length of PMS, the J_c of HIP'ed samples is not limited by granularity [32]. However there is evidence that in bulk PMS, the superconducting properties near the grain boundaries are degraded [12]. Hence our flux penetration results obtained in high AC and DC fields are consistent with those authors who conclude that PMS can be fabricated as a bulk pinning, homogenous superconductor.

As seen by other authors [33–35], the volume pinning force obeys a universal scaling law with the form of the Kramer dependence (Eq. (5)) similar to that commonly observed in Nb_3Sn. Since α is inversely proportional to the grain size in Nb_3Sn, grain boundaries are considered the major pinning centres. However there is no general agreement on the fundamental mechanism operating at the grain boundaries or the derivation of the Kramer dependence. Since a Kramer dependence and increasing J_c with decreasing grain size has also been found in PMS, a number of authors [36–38] have concluded that a grain boundary pinning mechanism operates. Consistent with preliminary SEM observations, we have found that HIP'ing the PMS at the relatively low temperature of 800°C increases the density by about 50% but there is no marked difference between the grain size of the HIP'ed and unHIP'ed PMS. Hence the increase in α by more than an order of magnitude can be attributed to an increase in the contact area between the grains, consistent with the reduction in porosity.

It is not yet established how to incorporate the irreversibility field into the Universal Fietz–Webb scaling laws. If the irreversibility line in PMS is attributed to thermal activation, the improvement in $\mu_0 H_{irr}$ in the HIP'ed PMS sample is due to a deeper potential well at the grain boundaries. Alternatively, if the properties of the grain boundaries are sufficiently extended on the scale of the coherence length, the region around the grain boundary may be considered to have a different local effective upper critical field. If in grain boundary pinning, the fluxons remain at the grain boundaries as they flow across the sample or if the pinning sites at the grain boundaries are effectively located in a region of superconductivity with a different upper critical field to the bulk, then the local upper critical field at the grain boundary may be the appropriate critical field to include in the universal scaling law. In general, HIP'ed materials have better bulk homogeneity, porosity and connectivity across grain boundaries. Hence it is unlikely that the HIP'ing has contributed to the reduction of the superconducting order parameter or equivalently deepened the pinning potential at the grain boundaries. In these materials, the improvements in $\mu_0 H_{irr}$ can be interpreted as an improvement in the effective upper critical field at the grain boundaries. For the HIP'ed PMS, $\mu_0 H_{irr}(T)$ lies very close to $\mu_0 H_{C2}(T)$ values determined from DC magnetisation and specific heat measurements on the same sample [11,39]. Hence the HIP'ed PMS has similar properties to the low temperature superconductors where experimentally there are only small differences between the upper critical field of the bulk and that of the grain boundaries.

Over a broad field range, the Kramer dependence is similar to an exponential pair-breaking field dependence of the form [40],

$$J_c = \alpha^*(T)\exp(-B/\beta^*(T)), \tag{6}$$

where $\alpha^*(T)$ and $\beta^*(T)$ are functions of temperature. This exponential functional form has been used to describe J_c in high temperature superconductors [41,42]. Equating Eq. (5) to Eq. (6) [40] gives,

$$\mu_0 H_{irr}(T) = 5\beta^*(T). \tag{7}$$

Hence in the context of Kramer's universal scaling law, the improved high field performance of the HIP'ed sample is due to an improvement in the effective upper critical field, or irreversibility field at the grain boundaries. Since over the field range for the measurements, the field dependence of J_c can be equally well described by Eq. (5) or Eq. (6), the improvement in the effective upper critical field at the grain boundaries may be explained by an increase in the characteristic decay field $\beta^*(T)$ at the grain boundaries.

Although HIP'ing has markedly improved the irreversibility line, the technological challenge of increasing J_c at fields between 20 and 30 T remains. Clearly experience optimising Nb_3Sn suggests that reduced grain size should be productive. The high $\mu_0 H_{irr}(T)$ values throughout the HIP'ed material suggest that increased pinning will also be required to achieve additional increases in J_c. Using a model assuming an optimal arrangement of pinning centres, where all flux lines are pinned [43], Rossel et al. [44] have estimated the maximum possible critical current density for PMS. They found it to be greater than $1 \times 10^{10}\,A\,m^{-2}$ at 4.2 and 20 T, at least one order of magnitude higher than the best experimental results. Rossel and Fischer have shown that artificially introducing pinning centres by neutron irradiation and the addition of fine non-superconducting particles in hot pressed samples can increase the J_c [45] indeed

intragranular current densities of up to 5×10^9 A m^{-2} at 4.2 K and 9 T [46,47] have been found. It is clear that J_c values have by no means reached an intrinsic upper limit.

6. Conclusion

A high quality HIP'ed PMS sample has been fabricated which has a T_c of 13.5 K, $\Delta T_c \approx 1$ K. Using XRD and SEM the sample has been shown to be single phase and close to fully dense. The magnetic moment of both an unHIP'ed and HIP'ed sample of PMS has been measured from 4.2 K up to T_c in DC magnetic fields up to 10 T. The results have been used to calculate the functional form and the spatial variation of J_c as a function of field and temperature.

The gradients of the magnetic fields profiles suggests that the spatial variation of J_c is small, indicating that both unHIP'ed and HIP'ed PMS can be considered as bulk pinning, homogenous superconductors. The J_c, scaling relations and pinning parameters of the HIP'ed sample compare well with DC magnetisation results. For both samples, the functional form of the volume pinning force obeys the universal Fietz–Webb scaling relation and can be expressed as $F_P \propto h^{1/2}(1-h)^2$, where h is the reduced field.

By processing the PMS using a HIP, the superconducting transition is sharper and T_c has increased by 1 K. J_c has increased by typically a factor of 20 to give a value greater than 4×10^8 A m^{-2} at 5 T and 6 K. The irreversibility line has also increased by a factor of almost 2 so that for HIP'ed PMS the irreversibility line lies very close to $\mu_0 H_{C2}(T)$ values determined by reversible DC magnetisation and specific heat measurements.

In the context of the universal scaling law for flux pinning, it is suggested that the marked increase in J_c produced by the HIP process is due to an increase in both the contact area between the grains and an increase in the irreversibility line. The improvement in the irreversibility line, which is attributed to improved superconducting properties at the grains boundaries. This can be explained by an increase at the grain boundaries in either the effective upper critical field or the characteristic decay field $\beta^*(T)$. This result opens the question as to the general efficacy of HIP'ing to improve the grain boundaries in other superconducting materials.

Acknowledgements

The authors wish to thank A. Crum (Engineered Pressure Systems, National Forge Europe) for use of the HIP, Dr. K. Durose (Department of Physics, University of Durham) for help with the SEM, Dr. C.W. Lehman (Department of Chemistry, University of Durham) for use of the XRD facilities and P.A. Russell (University of Durham) for help with the production of the diagrams. Financial support was provided by the EPSRC, UK and The Royal Society, UK.

References

[1] R. Chevrel, S. Sergent and J. Prigent, J. Solid State Chem. 3 (1971) 515.
[2] B.T. Matthias, M. Marezio, E. Lorenzwit, A.S. Cooper and H.E. Barz, Science 175 (1972) 1465.
[3] S. Foner, E.J. McNiff, Jr. and E.J. Alexander, Phys. Lett. 49A (1974) 269.
[4] S. Foner, E.J. McNiff, Jr. and E.J. Alexander, IEEE Trans. Magn. MAG-11 (1975) 155.
[5] D. Cattani, J. Cors, M. Decroux, B. Seeber and Ø. Fischer, Physica C 153–155 (1988) 461.
[6] J. Cors, D. Cattani, M. Decroux, A. Stettler and Ø. Fischer, Physica B 165 (1990) 1521.
[7] R. Odermatt, Ø. Fischer, H. Jones and G. Bongi, J. Phys. C 7 (1974) L13.
[8] R. Flükiger and B. Seeber, Europhys. News 22 (1991) 1.
[9] B. Seeber, M. Decroux and Ø. Fischer, Physics B 155 (1989) 129.
[10] R. Rossel, NATO ASI Relaxation in Complex Systems and Related Topics, eds. I.A. Campbell and C. Giovannella (Plenum, New York, 1989).
[11] D.N. Zheng, H.D. Ramsbottom and D.P. Hampshire, Phys. Rev. B 52 (1995) 12931.
[12] M. Decroux, P. Selvam, J. Cors, B. Seeber, Ø. Fischer, R. Chevrel, P. Rabiller and M. Sergent, IEEE Trans. Appl. Supercond. 3 (1993) 1502.
[13] A.M. Campbell, J. Phys C 2 (1969) 1492.
[14] H.D. Ramsbottom and D.P. Hampshire, Meas. Sci. Technol. 6 (1995) 1349.
[15] H.V. Atkinson and B.A. Rickinson, Hot Isostatic Processing, ed. J. Wood (Adam Hilger, Bristol, UK, 1991).
[16] E. Arzt, M.F. Ashby and K.E. Easterling, Metall. Trans. 14A (1983) 212.

[17] A.S. Helle, K.E. Easterling and M.F. Ashby, Acta Metall. 33 (1985) 2163.
[18] W.B. Li, M.F. Ashby and K.E. Easterling, Acta Metall. 35 (1987) 2831.
[19] W. Kaysser, M. Aslan, E. Arzt, M. Mitkov and G. Petzow, Powder Metall. 31 (1988) 63.
[20] H.D. Ramsbottom, D.N. Zheng and D.P. Hampshire, IEEE Trans. Appl. Supercond. 5 (1995) 1321.
[21] B. Seeber, L. Erbuke, V. Schroeter, J.A.A.J. Perenboom and R. Grill, IEEE Trans. Appl. Supercond. 5 (1995) 1205.
[22] P. Rabiller, M. Rabiller-Baudry, S. Even-Boudjada, L. Burel, R. Chevrel, M. Sergent, M. Decroux, J. Cours and J.L. Maufras, Mater. Res. Bull. 29 (1994) 567.
[23] H.D. Ramsbottom and D.P. Hampshire, J. Phys C (1996), submitted.
[24] C.P. Bean, Rev. Mod. Phys. 36 (1964) 31.
[25] A. Umezawa, G.W. Crabtree, J.Z. Liu, H.W. Weber, W.K. Kwok, L.H. Nunez, T.J. Moran and C.H. Sowers, Rev. Rev. B 36 (1987) 7151.
[26] E.J. Kramer, J. Appl. Phys. 44(3) (1973) 1360.
[27] C. Rossel, O. Peña, H. Schmitt and M. Sergent, Physica C 181 (1991) 363.
[28] V.R. Karasik, E.V. Karyaev, V.M. Zakasarenko, M.O. Rickel and V.I. Tsebro, Sov. Phys. JETP 60 (1984) 1221.
[29] D. Cattani, J. Cors, M. Decroux, B. Seeber and Ø. Fischer, Helv. Phys. Acta 63 (1990) 797.
[30] D. Cattani, J. Cors, M. Decroux and Ø. Fischer, Physica B 165 (1990) 1409.
[31] K. Kajiyana, T. Matsushita, K. Yamafuji, K. Hamasaki and T. Komata, Jpn. J. Appl. Phys. 25 (1986) 831.
[32] L. Le Lay, T.C. Willis and D.C. Larbalestier, Appl. Phys. Lett. 60 (1992) 775.
[33] S.A. Alterovitz and J.A. Woollam, Philos. Mag. B 38 (1978) 619.
[34] Y. Kimura, Phys. Status Solidi (a) 69 (1982) K189.
[35] V.R. Karasik, E.V. Karyaev, M.O. Rickel and V.I. Tsebro, Sov. Phys. JETP 56 (1982) 881.
[36] M.O. Rikel, T.G. Togonidze and V.I. Tsebro, Sov. Phys. Solid State 28 (1987) 1496.
[37] A. Gupta, M. Decroux, P. Selvam, D. Cattani, T.C. Willis and Ø. Fischer, Physica C 234 (1994) 219.
[38] L.A. Bonney, T.C. Willis and D.C. Larbalestier, IEEE Trans. Appl. Supercond. 3 (1993) 1582.
[39] S. Ali, H.D. Ramsbottom and D.P. Hampshire, in: EUCAS'95, Inst. Phys. Conf. Ser. 148 (1995) 583.
[40] D.P. Hampshire, Applied Superconductivity, ed. H.C. Freyhardt (DGM Informationsgesellschaft, 1993) p. 23.
[41] L. Le Lay, C.M. Friend, T. Maruyama, K. Osamura and D.P. Hampshire, J. Phys C 6 (1994) 10063.
[42] K. Osamura, S. Nonaka, M. Matsui, T. Oku, S. Ochiai and D.P. Hampshire, J. Appl. Phys. 79(10) (1996) 7877.
[43] E.H. Brandt, Phys. Lett. 77 A (1980) 484.
[44] C. Rossel, E. Sandvold, M. Sergent, R. Chevrel and M. Potel, Physica C 165 (1990) 233.
[45] C. Rossel and Ø. Fischer, J. Phys. F 14 (1984) 455.
[46] A. Gupta, N. Cheggour, M. Decroux, V. Bouquet, P. Langlois, H. Massat, R. Flükiger and Ø. Fischer, Physica C 235–240 (1994) 2543.
[47] D. Cattani, Thesis Universite Geneve PhD (1980).